

Archive ouverte UNIGE

https://archive-ouverte.unige.ch

Article scientifique

Article

2020

Accepted version

Open Access

This is an author manuscript post-peer-reviewing (accepted version) of the original publication. The layout of the published version may differ .

A Solid-State Reference Electrode Based on a Self-Referencing Pulstrode

Gao, Wenyue; Zdrachek, Elena; Xie, Xiaojiang; Bakker, Eric

How to cite

GAO, Wenyue et al. A Solid-State Reference Electrode Based on a Self-Referencing Pulstrode. In: Angewandte Chemie: International Edition, 2020, vol. 59, n° 6, p. 2294–2298. doi: 10.1002/anie.201912651

This publication URL: https://archive-ouverte.unige.ch/unige:136738

Publication DOI: <u>10.1002/anie.201912651</u>

© This document is protected by copyright. Please refer to copyright holder(s) for terms of use.

A Solid-State Reference Electrode Based on a Self-Referencing Pulstrode

Wenyue Gao, [a,b] Elena Zdrachek, [a] Xiaojiang Xie, *,[b] and Eric Bakker*,[a]

Abstract: The design of solid-state reference electrodes without liquid junction is of great importance to allow for miniature and costeffective electrochemical sensors in environmental and biomedical applications. To address this, we propose here a pulse control protocol using an Ag/AgI element as reliable solid-state reference electrode. It involves the local release of iodide by a cathodic current that is immediately followed by an electromotive force (EMF) measurement that serves as the reference potential. The recapture of iodide ions is achieved by potentiostatic control. This results in intermittent potential values that are reproducible to less than one millivolt (SD = 0.27 mV, n = 50). The ionic strength is shown to influence the activity coefficient of released iodide in accordance with the Debye-Hückel equation, resulting in a predictable change of the potential reading. The principle is applied to potentiometric potassium detection with a valinomycin-based ion-selective electrode (ISE), demonstrating a completely solid-state sensor configuration. The resulting calibration curves compare quantitatively to a commercial liquid junction-based reference electrode, even in spiked artificial sweat samples. This approach offers a promising strategy to the design of all-solid-state electrochemical sensing probes.

The design and fabrication of solid-state reference electrodes that are easily miniaturized and cost-effective for mass production is becoming increasingly important for the realization of compact sensing devices. Indeed, there is a growing demand for wearable sensors and point-of-care tests^[1] to provide real-time information of health parameters, and many of these systems are operated electrochemically.^[2] However, the accuracy and precision of electrochemical measurements strongly depends on the stability and reproducibility of the reference electrode potential.^[3] Traditional reference electrodes typically contain a reference element (Ag/AgCI) and an aqueous reference solution that is separated from the sample solution by a porous diaphragm.^[4] As this is a cumbersome design, it is highly desirable to replace this reference electrode with an all-solid-state miniaturized system.

In a most conservative approach, research has focused on developing reference electrodes with solidified reference electrolytes (most commonly KCI) in the form of a melt, gel or a polymer matrix.^[5] In these approaches, the liquid junction potential between the reference electrode and sample solutions

[a] Dr. W. Gao, Dr. E. Zdrachek, Prof. E. Bakker Department of Inorganic and Analytical Chemistry University of Geneva Quai Ernest-Ansermet 30, CH-1211 Geneva, Switzerland E-mail: eric.bakker@uniqe.ch

[b] Dr. W. Gao, Prof. X. Xie Department of Chemistry Southern University of Science and Technology Shenzhen 518055, China

E-mail: xiexj@sustech.edu.cn

Supporting information for this article is given via a link at the end of the document.

is maintained by the slow leaching of the reference electrolyte. Such reference electrodes are environmentally friendly and easy to miniaturize, but the resulting lifetime becomes limited upon miniaturization owing to geometrical constraints.^[3] The lifetime may be extended by embedding the reference electrolyte into highly cross-linked polymers, but this may result in a high resistance and long equilibration time.^[6]

Ionic liquid (IL)-based reference electrodes without liquid junction offer a viable alternative over conventional KCI-based reference electrodes.[7] Upon contact with an aqueous phase, a distribution equilibrium is formed between two immiscible phases caused by the finite solubility of the IL in water.[8] A stable interfacial potential across these two phases may form that is determined by the partitioning of the ionic liquid salt, provided that ionic species in the aqueous solution exhibit negligible solubility in the IL phase.[9] Distinct advantages[10] include high stability even in weakly buffered and low ionic strength solutions, [9b, 11] while the potential of commercial reference electrodes with porous frits may change with the sample composition and frit material.[12] Disadvantages include a limited lifetime upon miniaturization owing to continuous leakage of the IL,[13] and an associated possible biotoxicity. Also, when applied to ion sensing with ion-selective membrane-based sensors, this same leakage may poison the ISE membrane owing to its relatively high lipophilicity. A recent review on the topic^[14] described various factors influencing the performance of IL-based reference electrodes, such as the chemical composition and purity of IL, the form of the IL-based membrane and its composition, and the experimental conditions used for measurement.

We propose here a truly solid-state reference electrode concept to obtain accurate intermittent potential readings, primarily targeted to potentiometric sensing purposes. It relies on a self-referencing protocol in which a current pulse generates ions at the electrode surface. These ions then dictate the electrode potential during a subsequent measurement step at zero current. A conceptually similar concept was introduced by Buhlmann with ion-selective polymeric membranes containing a hydrophobic salt, where a current pulse released a hydrophobic ion from the membrane to stabilize the potential.[15] Unfortunately, the high resistance of these membranes, dictated by low ion mobilities, limits the imposable current density and the applicability of the approach. Moreover, this principle has not been demonstrated in an all-solid-state configuration. To overcome these limitations, a low resistance, solid-state Ag/AgI electrode is used here as reference electrode by pulse control. The iodide ions determining the potential of the electrode are produced in-situ and may be recaptured, thus providing independent and reproducible potentials. An Agl solid-state electrode may achieve a high concentration of the released ions that can be tuned with the applied current pulse. They exhibit a much lower electrical resistance and should not be concerned by undesired membrane concentration polarizations while releasing the ions.

The Ag/Agl electrode is readily prepared by depositing an Agl layer onto a silver electrode surface under galvanostatic control (see Experimental procedures in SI). The expected Nernstian response of the Ag/AgI electrode to different concentrations of iodide ions was observed (Figure S1). The associated constant potential contribution (E0) was used for theoretical simulations. The automated measurement sequence involved the recording of the initial open circuit potential (OCP) in the solution of interest. The triple pulse steps were then executed as follows for each measurement point: iodide was locally released by applying a constant cathodic current pulse; the EMF was subsequently recorded at open-circuit; the released iodide ions were recaptured by applying a constant potential pulse based on the initial OCP value. The processes occurring during the sequence are schematically shown in Figure 1a while Figure 1b traces the potential during the electrochemical protocol, with the blue dot indicating the potential reading used for the actual measurement. Figure 1c shows the simulated time-dependent iodide ion concentration profiles near the Ag/AgI electrode surface for each pulse at 0.5 s intervals. As the iodide concentration increases during the galvanostatic step, the potential of the electrode decreases. Immediately after the first step, the EMF is measured. The small potential jump from the last point in the galvanostatic step to the first point in the EMF detection step indicates the ohmic drop of the electrochemical cell, which is eliminated during pulse II. As iodide ions continue to diffuse away from the electrode surface during pulse II, the EMF value is expected to increase by ca. 11 mV in the first second. However, before the iodide ions diffuse too far into the bulk sample solution, they are recaptured under a potentiostatic pulse. The potential of this reference electrode relies on the concentration of iodide released in-situ from the AgI layer during the galvanostatic pulse, assuming that no iodide or other interfering species such as sulfide are present in bulk solution. lodide is indeed not common in most samples. Note that Ag/AgI is sensitive to light and should be kept in the dark during measurement.[16] The pulse-based self-referencing protocol is versatile and may be executed with other electrochemical systems.

To obtain reproducible and stable EMF values, the conditions for the three control steps were optimized, including the amplitude and length of the applied current in the iodide release step, the regeneration potential and length in the third step (details in SI from Figure S2 to S6). In brief, with increasing amplitude and length of the applied current, more iodide ions were released, thus leading to more negative reference potentials. For an electrode with a diameter of 3 mm, the following conditions were adopted with a current pulse of -5 μA for 5s, and with the optimum regeneration potential of OCP plus 50 mV for 30 s.

The potential value used as the final reference electrode signal was measured at open-circuit for a period of 1-s at sampling interval of 25 ms. In principle, any point during this period may be used for analysis. The EMF values measured at open-circuit during the 1-s period from 50 measurements are shown in Figure S7. The last points gave a somewhat higher standard deviation of 0.39 mV compared with that of the initial

reading of 0.27 mV, and so the first reading during the EMF pulse was chosen in subsequent work.

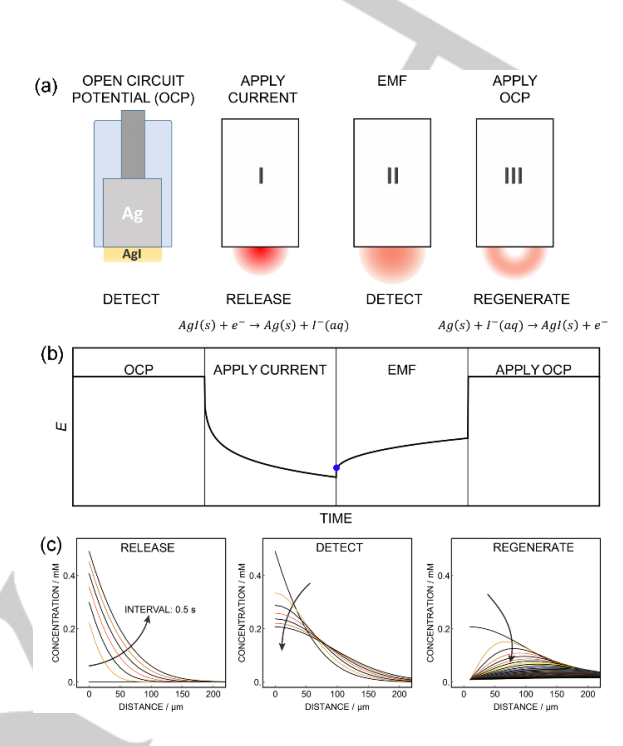


Figure 1. The schematic illustrations of the working principle (a), the potential change (b) and iodide concentration change (c) during the pulse steps.

The triple pulse steps were then executed with the optimized conditions. Three typical consecutive time-dependent data are shown in Figure 2 when recorded vs. a commercial reference electrode (Ag/AgCl/3 M KCl/1 M LiOAc). This involved an applied current of -5 μA for 5-s (step I), the EMF reading for 1-s (step II) and an applied constant potential at OCP + 50 mV for 30-s (step III). The theoretically simulated and experimental current-time curves and potential-time curves show excellent agreement, see Figure S8.

The variability of the intermittent potential readings (blue dots in Figure 2) for different concentrations of NaCl solutions was evaluated. As shown in Figure 3a, a potential increase of about 4 mV was observed as the concentration of NaCl increased from 10 to 150 mM, which is ascribed to the increasing ionic strength. According to the Nernst equation, the potential of the electrode depends on the activity of iodide, not its concentration. As the applied current pulse releases a certain quantity over time that translates into a predetermined concentration, increasing ionic strength should result in a lower activity for the same concentration, and hence in a higher potential reading. The red line in Figure 3 shows the expected potential change from increasing ionic strength as calculated by the extended Debye-Hückel equation (Eqn. S8), which corresponds well to the experimental results. When subtracting the theoretically calculated data from each experimental point, an average residual of 0.22 mV for the variation in background concentration was obtained (Figure 3b), with errors ranging from

0.08~mV to 0.30~mV (SD, n=3). This suggests that the potential reading can be readily corrected if the ionic strength of the solution is known.

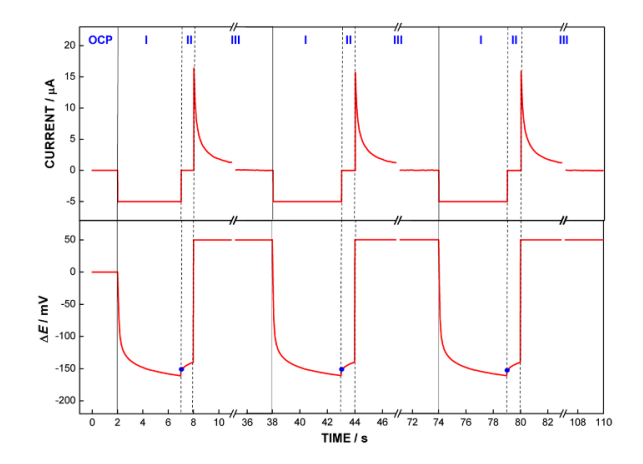


Figure 2. The experimental current-time curves and potential-time curves for the pulse control steps: (I) applying a constant current of -5 μ A for 5 s; (II) the EMF measurement for 1 s; (III) applying a constant recapture potential based on the original OCP value of the electrode (OCP plus 50 mV) for 30 s. The blue dots are chosen for analysis.

The common multivalent anions sulfate and phosphate were also investigated to explore their influence on the reference potential. As shown in Figure S9 and Figure S10, a potential difference of about 2 mV and 1 mV, respectively, was observed in a 0.1 M NaCl background electrolyte with increasing concentration of sulfate and phosphate buffer up to 0.1 M. This moderate potential difference also originates from the decreasing activity coefficient of iodide with increasing ionic strength, in analogy to Figure 3. The experimental results agree with the behavior calculated from the extended Debye-Hückel equation. The common anions sulfate and phosphate do not interfere with the release and recapture of iodide. The adoption of this Ag/Agl pulstrode in common buffers should not be problematic.

This new reference protocol is promising for the design of wearable sensors. Potassium is an indispensable ionic species that plays a key role in a range of physiological processes^[17] and should be maintained in the normal range. As the monitoring of potassium in sweat may help to assess the physiological state of the subject, recent work has been devoted to achieving the real-time potassium detection in sweat using wearable sensors.^[18]

Combined with a valinomycin-based ion-selective membrane as all-solid-state potassium probe, the performance of the selfdifferent referencing electrode investigated in was concentrations of NaCl background solutions. The threeelectrode configuration of the detection cell with a platinum counter electrode is shown in Figure 4a. To allow for the current to pass through the pulstrode, the Ag/AgI element was connected to the working electrode input and the potassium probe to the reference input of the potentiostat. To keep with standard practice, the sign of the obtained data was subsequently reversed. The observed calibration curves of EMF against the logarithmic potassium activity for different NaCl background concentrations are shown in Figure 4b. The EMF values were corrected by subtracting the influence of the ionic strength on the activity of released iodide (see also Figure 3). In a separate experiment, a commercial reference electrode (Ag/AgCl/3 M KCl/1 M LiOAc) was used instead (Figure S11). For the proposed Ag/AgI reference pulstrode a mean Nernstian slope of 58.0 mV/decade (SD: 0.68 mV) was found, which compares well to the slope of 56.8 mV/decade (SD: 0.55 mV) for the commercial reference electrode.

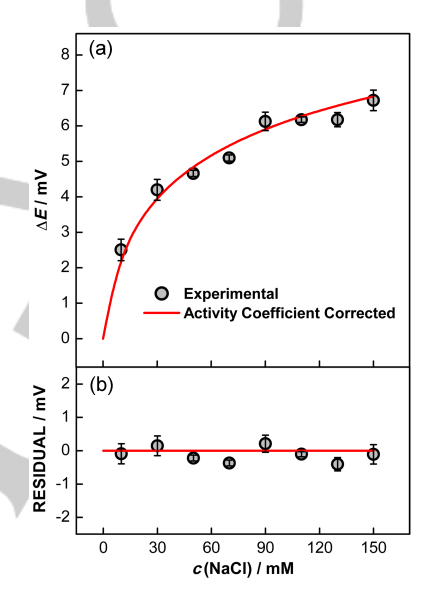


Figure 3. (a) Experimental potential deviations (n=3) and theoretical potential change (red line) taking into account the change of iodide activity coefficient by increasing ionic strength (NaCl concentration), and (b) the residual values. The experimental potential readings were corrected by the junction potential from the conventional reference electrode of Ag/AgCl/3 M KCl/1 M LiOAc used here.

Potassium detection in spiked artificial sweat samples was carried out to further prove the applicability of the reference pulstrode approach to real samples. Comparable Nernstian slopes of 56.1 mV/decade and 55.8 mV/decade were successfully achieved in the physiological concentration range of 1 mM to 10 mM using the proposed Ag/AgI pulstrode (Figure 4c) and a commercial Ag/AgCI reference electrode (Figure S12), respectively. The performance is comparable, suggesting that the approach introduced here is promising.

We note that the reference potential based on this Ag/Agl pulstrode is dependent on the diffusion coefficient of the released iodide from the electrode surface. This should depend on the viscosity of the sample solution and the temperature according to the Stokes-Einstein theory^[19] (Equation S14 in Supporting Information). The viscosity of human sweat, for example, ranges from 0.9 to 1.2 cP at 30 °C.^[20] The reference potential difference caused by this viscosity change is calculated to be ca. 3.8 mV, which may be acceptable for monitoring purposes but should be considered in precise requirements. If

so, a protective gel layer on the electrode surface may eliminate viscosity variations from the sample composition, as successfully demonstrated by Buffle.^[21]

This principle is primarily targeted to potentiometric sensors, providing discrete measurement points at certain time intervals. It is not directly suited for continuous measurements or for dynamic electrochemistry where the potential must be controlled over a measurement period. However, this is achievable in combination with a pseudo-reference element^[22] that is stable

over time and whose potential reading can be corrected with the pulsed reference electrode. This is demonstrated with the continuous potentiometric detection of potassium as example, which were sequentially corrected with the pulstrodes approach introduced here. The potential readings with the pseudoreference electrode are initially not accurate, but match the potential changes with a conventional reference electrode after correction with the proposed pulstrode (Figure S13).

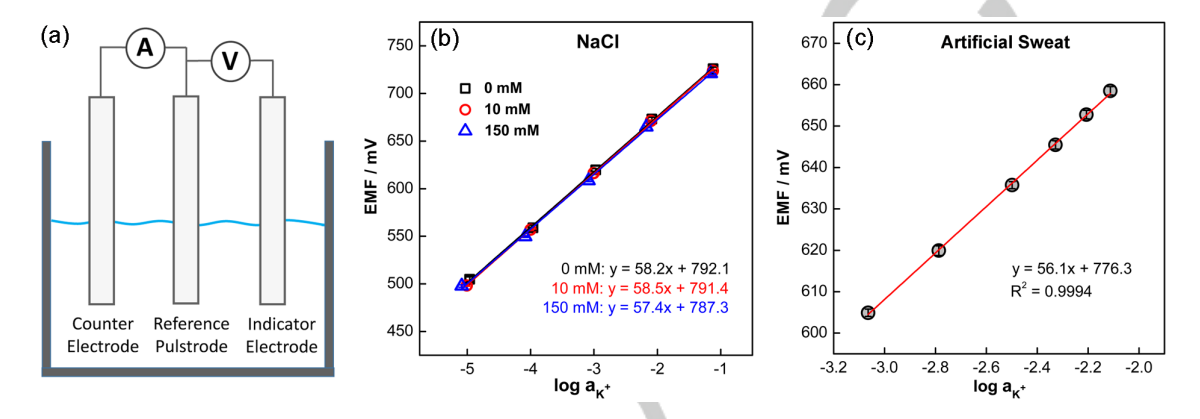


Figure 4. (a) Configuration of the detection cell consisting of a Pt counter electrode, an Ag/AgI reference pulstrode, and a solid-state potassium-selective indicator electrode. Calibration curves for potassium detection based on the Ag/AgI solid-state reference pulstrode (b) in different concentrations of NaCI solutions and (c) in spiked artificial sweat samples. In both cases, n=9, with 3 electrodes repeated 3 times each.

In conclusion, a self-referencing protocol based on a pulstrode approach is proposed here using Ag/AgI as a readily available solid-state reference electrode. It provides an alternative to reference electrodes with reliable stability and reproducibility. Theoretical simulations and experimental results verified the feasibility of this approach. It shows good stability and comparable performance with KCI-based commercial reference electrodes when applied to potassium detection with various electrolyte backgrounds. The approach appears to work even in relatively low ionic strength solutions, although one might expect electrical migration at very low ionic strength to give distorted concentration profiles and hence different potential readings. A prerequisite of the approach is that the local concentration of the released ion should be much higher than the basal level in solution, and that interfering ions such as sulfide are absent. The observed reference potential is dependent on the activity of iodide at the electrode/solution interface, and therefore also depends on the diffusion coefficient of iodide and hence on sample viscosity and temperature. If required, this may be addressed with protective hydrogel layers on the electrode surface. It is also noted that this principle provides a discrete measurement point at certain time intervals and is therefore not directly useful for dynamic measurements. but it can be achieved in combination with a pseudo-reference element that is stable over time and whose potential reading can be corrected with the pulsed reference electrode. In this manner, the pulstrode approach offers an alternative strategy to the design of all-solid-state electrochemical sensing probes and may

facilitate the realization of reliable wearable sensors and pointof-care testing devices.

Acknowledgements

We thank the Swiss National Science Foundation (200021_175622) and the National Natural Science Foundation of China (21874063) for financial support.

Keywords: reference electrode • potential • silver iodide • pulstrode • electrochemical sensors

- [1] a) J. Hu, A. Stein, P. Bühlmann, *TrAC-Trend. Anal. Chem.* 2016, 76, 102-114; b) J. Hu, W. Zhao, P. Bühlmann, A. Stein, *ACS Appl. Nano Mater.* 2018, 1, 293-301.
- [2] a) J. Kim, A. S. Campbell, B. E.-F. de Ávila, J. Wang, Nat. Biotechnol.
 2019, 37, 389-406; b) Y. Yang, W. Gao, Chem. Soc. Rev. 2019, 48, 1465-1491; c) A. J. Bandodkar, J. Wang, Trends Biotechnol. 2014, 32, 363-371; d) Y. Dai, C. C. Liu, Angew. Chem. Int. Ed. 2019, 58, 12355-12368; e) P. B. Luppa, C. Müller, A. Schlichtiger, H. Schlebusch, TrAC-Trend. Anal. Chem. 2011, 30, 887-898.
- [3] U. Guth, F. Gerlach, M. Decker, W. Oelßner, W. Vonau, J. Solid State Electrochem. 2009. 13. 27-39.
- [4] a) R. K. Nagarale, U. Hoss, A. Heller, J. Am. Chem. Soc. 2012, 134, 20783-20787; b) R. Kalidoss, A. S. Raja, D. Jeyakumar, N. Prabu, IEEE Sens. J. 2018, 18, 8510-8516.
- [5] a) Z. Mousavi, K. Granholm, T. Sokalski, A. Lewenstam, Analyst 2013, 138, 5216-5220; b) J. Ding, B. Li, L. Chen, W. Qin, Angew. Chem. Int. Ed. 2016, 55, 13033-13037; c) A. Lewenstam, T. Blaz, J. Migdalski, Anal. Chem. 2017, 89, 1068-1072.

- [6] J. Bobacka, Anal. Chem. 1999, 71, 4932-4937.
- [7] T. Kakiuchi, Electrochem. Commun. 2014, 45, 37-39.
- [8] a) M. Armand, F. Endres, D. R. MacFarlane, H. Ohno, B. Scrosati, Nat. Mater. 2009, 8, 621; b) T. Kakiuchi, N. Tsujioka, S. Kurita, Y. Iwami, Electrochem. Commun. 2003, 5, 159-164.
- [9] a) M. Shibata, M. Yamanuki, Y. Iwamoto, S. Nomura, T. Kakiuchi, Anal. Sci. 2010, 26, 1203-1206; b) S. A. Chopade, E. L. Anderson, P. W. Schmidt, T. P. Lodge, M. A. Hillmyer, P. Bühlmann, ACS Sens. 2017, 2, 1498-1504.
- [10] L. Zhang, T. Miyazawa, Y. Kitazumi, T. Kakiuchi, Anal. Chem. 2012, 84, 3461-3464.
- [11] Y. Kudo, M. Shibata, S. Nomura, N. Ogawa, Anal. Sci. 2017, 33, 739-742.
- [12] a) M. P. S. Mousavi, S. A. Saba, E. L. Anderson, M. A. Hillmyer, P. Bühlmann, *Anal. Chem.* 2016, 88, 8706-8713; b) K. Schwabe, H. D. Suschke, *Angew. Chem. Int. Ed.* 1964, 3, 36-46.
- [13] X. U. Zou, P. Bühlmann, Anal. Chem. 2013, 85, 3817-3821.
- [14] E. Lindner, M. Guzinski, T. A. Khan, B. D. Pendley, ACS Sens. 2019, 4, 549-561
- [15] a) S. Makarychev-Mikhailov, A. Shvarev, E. Bakker, J. Am. Chem. Soc. 2004, 126, 10548-10549; b) K. L. Gemene, M. E. Meyerhoff, Anal. Chem. 2010, 82, 1612-1615.

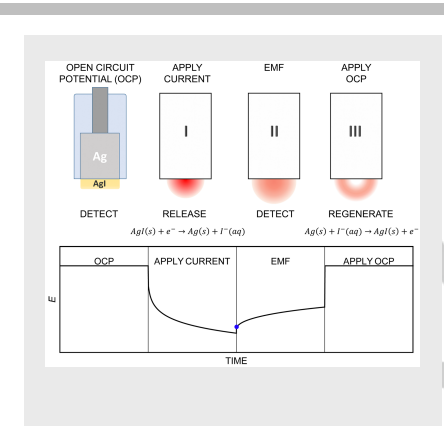
- [16] H. Cheng, B. Huang, Y. Dai, X. Qin, X. Zhang, Langmuir 2010, 26, 6618-6624.
- [17] a) F. Baixauli, M. Villa, E. L. Pearce, *Science* 2019, 363, 1395-1396; b)
 D. J. Jung, J. Y. Lee, K. H. Cho, K.-Y. Lee, J. Y. Do, S. H. Kang, *Sci. Rep.* 2019, 9, 9694; c) A. Rozov, I. Khusainov, K. El Omari, R. Duman, V. Mykhaylyk, M. Yusupov, E. Westhof, A. Wagner, G. Yusupova, *Nat. Commun.* 2019, 10, 2519.
- [18] a) W. Gao, S. Emaminejad, H. Y. Y. Nyein, S. Challa, K. Chen, A. Peck, H. M. Fahad, H. Ota, H. Shiraki, D. Kiriya, D.-H. Lien, G. A. Brooks, R. W. Davis, A. Javey, *Nature* 2016, 529, 509; b) M. Bariya, H. Y. Y. Nyein, A. Javey, *Nat. Electron.* 2018, 1, 160-171.
- [19] J. Brillo, A. I. Pommrich, A. Meyer, Phys. Rev. Lett. 2011, 107, 165902.
- [20] H. M. Emrich, E. Stoll, B. Friolet, J. P. Colombo, R. Richterich, E. Rossi, Pediat. Res. 1968, 2, 464-478.
- [21] a) M. L. Tercier, J. Buffle, Anal. Chem. 1996, 68, 3670-3678; b) M.-L. Tercier-Waeber, F. Confalonieri, M. Koudelka-Hep, J. Dessureault-Rompré, F. Graziottin, J. Buffle, Electroanalysis 2008, 20, 240-258.
- [22] E. Grygolowicz-Pawlak, G. A. Crespo, M. G. Afshar, G. Mistlberger, E. Bakker, Anal. Chem. 2013, 85, 6208-6212.

Entry for the Table of Contents (Please choose one layout)

Layout 1:

COMMUNICATION

A solid-state reference electrode principle is proposed here that relies on a self-referencing Ag/AgI element. An applied current pulse generates iodide ions that dictate the reference electrode potential, which are subsequently recaptured.



Wenyue Gao, Elena Zdrachek, Xiaojiang Xie,* and Eric Bakker*

Page No. – Page No.

A Solid-State Reference Electrode Based on a Self-Referencing Pulstrode

Supporting Information ©Wiley-VCH 2016 69451 Weinheim, Germany

A Solid-State Reference Electrode Based on a Self-Referencing Pulstrode

Wenyue Gao, Elena Zdrachek, Xiaojiang Xie,* and Eric Bakker*

Abstract: The design of solid-state reference electrodes without liquid junction is of great importance to allow for miniature and cost-effective electrochemical sensors in environmental and biomedical applications. To address this, we propose here a pulse control protocol using an Ag/Agl element as reliable solid-state reference electrode. It involves the local release of iodide by a cathodic current that is immediately followed by an electromotive force (EMF) measurement that serves as the reference potential. The recapture of iodide ions is achieved by potentiostatic control. This results in intermittent potential values that are reproducible to less than one millivolt (SD = 0.27 mV, n = 50). The ionic strength is shown to influence the activity coefficient of released iodide in accordance with the Debye-Hückel equation, resulting in a predictable change of the potential reading. The principle is applied to potentiometric potassium detection with a valinomycin-based ion-selective electrode (ISE), demonstrating a completely solid-state sensor configuration. The resulting calibration curves compare quantitatively to a commercial liquid junction-based reference electrode, even in spiked artificial sweat samples. This approach offers a promising strategy to the design of all-solid-state electrochemical sensing probes.

DOI: 10.1002/anie.2016XXXXX

Table of Contents

Experimental Procedures	3
Results and Discussion	4
Theoretical simulations	4
Figure S1. Observed Nernstian response of Ag/Agl electrode to different activities of iodide ions	6
Figure S2. Dependence of the EMF value on the applied current in galvanostatic step	6
Figure S3. Dependence of the EMF value on the time of the applied current in galvanostatic step	7
Figure S4. The linear sweep voltammetry of the Ag/Agl electrode in 100 mM of NaCl solution containing 10 mM of NaI	7
Figure S5. The dependence of Ag/AgI electrode stability on the regeneration potential	8
Figure S6. The dependence of Ag/AgI electrode stability on the regeneration time	9
Figure S7. The potential values measured at open-circuit in one second	9
Figure S8. The simulated and experimental curves for the pulse control steps	10
Figure S9. The influence of sulfate on the reference potential of the Ag/AgI pulstrode	10
Figure S10. The influence of phosphate species on the reference potential of the Ag/AgI pulstrode	11
Figure S11. The calibration curves for potassium detection using conventional reference electrode in different concentrations of NaCl solutions	11
Figure S12. The calibration curve for potassium detection using conventional reference electrode in spiked artificial sweat samples	12
Figure S13. Time responses and relative calibration curves for continuous potentiometric measurements with a pseudo-reference electrode	12
References	12
Author Contributions	12

Experimental Procedures

Reagents. Sodium tetrakis[3,5-bis(trifluoromethyl)-phenyl]borate (NaTFPB), valinomycin (potassium ionophore I), tetrakis(4-chlorophenyl)borate tetradodecylammonium salt (ETH 500), poly(vinyl chloride) (PVC), bis(2-ethylhexyl)sebacate (DOS), poly(3-octylthiophene) (POT), sodium iodide (NaI), sodium chloride (NaCI), potassium chloride (KCI), and tetrahydrofuran (THF) were purchased from Sigma-Aldrich and used as received. Urea was bought from Merck and lactic acid (90%) was from Fluka. Nafion membrane NR-211 of a thickness of 25 µm was obtained from Ion Power (Inc. 720 Governor Lea Rd, New Castle, DE19720).

Electrochemical Equipment and Electrode Preparation. The electrochemical measurements were carried out with an Autolab PGSTAT128N (Metrohm Autolab, Utrecht, The Netherlands) controlled by a personal computer using Nova 2.1.4 software (supplied by Autolab). A platinum electrode (6.0331.010 model, Metrohm, Switzerland) was used as counter electrode. A double-junction Ag/AgCl/3 M KCl/1 M LiOAc reference electrode (6.0726.100 model, Metrohm, Switzerland) was used as a comparison. The Ag/Agl electrode was prepared by electrochemically depositing an Agl layer on the surface of an Ag electrode (6.1204.330 model with a diameter of 3.0 mm, Metrohm, Switzerland) in a solution of 0.1 M Nal for one hour at a constant current density of 0.5 mA cm⁻². A glassy carbon (GC) electrode with a diameter of 3.0 mm (Model 6.1204.300) purchased from Metrohm (Switzerland) was used as inner electrode for solid-contact ion-selective electrode (ISE). Before use, it was polished with 0.3 μm alumina and washed with water. POT was deposited onto the GC discs by drop-casting 10 μL of a 0.25 mM solution (calculated with respect to the monomer) in chloroform.^[1] After a few minutes of drying, a membrane cocktail solution for potassium determination was drop cast onto the POT GC electrode. The membrane cocktail solution was prepared by dissolving 100 mg of components in 1.0 mL THF^[2]: 15 mmol/kg of valinomycin, 5 mmol/kg NaTFPB, 30 mmol/kg ETH 500, 31.5 mg of PVC and 63 mg of DOS. A volume of 150 μL of the cocktail (3x50 μL) was pipetted and drop cast on the POT GC electrode. A pseudo-reference electrode consisting of a Nafion membrane was prepared according to a previous paper,^[3] and was applied into continuous potentiometric measurements providing potentials that can be calibrated by the Ag/AgI pulstrode in a separate step.

Preparation of the artificial sweat sample. The composition of the artificial sweat corresponds to DIN 53160-2 norm and contains the typical pH value of sweat and the common concentrations of sweat ingredients including urea, lactic acid, ammonium and sodium chloride. It was prepared as follows: 0.5 g of urea, 2.5 g of sodium chloride and 0.5 g of lactic acid were added into a beaker, followed by the addition of 450 mL of water to dissolve all the reagents. Ammonium hydroxide solution (1%) was added until a stable pH value of 6.5 was achieved. The solution was transferred into a 500 mL volumetric flask and filled with water up to the mark. Before use, the pH of the sweat simulant was verified to be around 6.5±0.1. We used this artificial sweat for potassium sensing by adding a defined amount of potassium ions to this solution.

Results and Discussion

Theoretical simulations

Simulations for the triple pulse control steps:

Theoretical simulations were made to predict the signals during the triple pulse control steps. In the first step, the local release of iodide by applying a constant cathodic current was calculated. Under a proper cathodic galvanostatic pulse, AgI is reduced to Ag and iodide ions (I^-) are released and diffuse away from the electrode surface in direction of the bulk solution. The diffusional flux of I^- relates to the applied current based on the Fick's first law:

$$i = nFAI_{I} \tag{S1}$$

where i is the applied current, A is the electrode surface area and n is the number of transferred electrons (n = 1), while F is the Faraday constant. Assuming that the electrochemical reaction is sufficiently fast and one-dimensional diffusion is the predominant form of mass transport, the ion flux J_I at the sample-electrode interface (x = 0) can be described as follows (D_I corresponds to the diffusion coefficient of iodide):

$$J_{I} = -D_{I} \left[\frac{\partial c_{I}(x,t)}{\partial x} \right]_{x=0}$$
 (S2)

The continuity equation (Eqn. S3) is used to quantify the time-dependent concentration changes for the subsequent time step:^[4]

$$\frac{\partial c_I(x,t)}{\partial t} = D_I \frac{\partial^2 c_I(x,t)}{\partial x^2} \tag{S3}$$

A finite difference method with equally spaced distance and time elements $(d, \Delta t)$ is now applied to discretize the concentration change: [5]

$$c_I(x, t + \Delta t) = c_I(x, t) + \frac{\Delta t}{d^2} D_I[c_I(x - 1, t) - 2c_I(x, t) + c_I(x + 1, t)]$$
(S4)

Once the initial conditions for the experiments in all elements of distance d are defined, the applied current amplitude is used to calculate the time independent concentration gradient at position 0 near the electrode surface, while all other concentrations for the next time step can be derived from Eqn. S4. The associated potential was then obtained based on the Nernst equation from the concentration (strictly, activity a_I) at position 0 (electrode surface):

$$E(t) = E_{AgI/Ag}^{0'} - \frac{RT}{F} \log c_I(0, t)$$
 (S5)

Subsequently, the potential at open-circuit (OCP) was predicted. The potential of the electrode relies on the concentration of iodide released from the AgI layer during the galvanostatic pulse. Diffusion of iodide ions from the electrode surface to the sample solution is assumed to be the dominant process. Taking the last element in the galvanostatic step above as the first element of this step, the concentration change was simulated based on the same equation (Eqn. S4), using a reflection at the electrode surface instead of the constant gradient assumed in step I. The potential change was then again calculated with Eqn. S5.

In the last step, the recapture of iodide ions under a potentiostatic pulse was simulated. Upon application of an appropriate anodic potential, Ag will be oxidized to produce AgI on the electrode surface with the previously released iodide. The magnitude of the applied potential defines the concentration of iodide ions at the electrode surface on the basis of the Nernst equation, which is chosen to be fixed in the calculation. The concentration change was otherwise simulated again according to Eqn. S4. Based on Fick's first law, the current change was obtained from the flux of iodide ions as follows:

$$i(t) = nFAJ_I(t) = -FAD_I \frac{\left(c_I(1,t) - c_I(0,t)\right)}{d} \tag{S6}$$

Activity coefficient calculation:

The activity of iodide a_I is related to the molar concentration c_j , through the activity coefficient γ_- , as follows:

$$a_I = \gamma_- c_I \tag{S7}$$

The mean activity coefficients were calculated on the basis of the extended Debye-Hückel theory:

$$log\gamma_{\pm} = -\frac{A|z_{+}z_{-}|\sqrt{I}}{1 + B\sqrt{I}} + CI$$
 (S8)

where A is a constant (A = 0.5108) that is a function of temperature in Kelvin, B and C are two parameters depending on the electrolyte in question, $^{[6]}$ while I represents the ionic strength for all ions j present in solution:

$$I = 0.5 \sum_{i} z_i^2 c_i \tag{S9}$$

The relevant single ion activity coefficient was calculated from the mean activity coefficient according to the simplified Debye-Hückel convention:

$$log\gamma_{+} = \left| \frac{Z_{+}}{Z} \right| log\gamma_{\pm} \tag{S10}$$

$$log\gamma_{-} = \left| \frac{Z_{-}}{Z_{+}} \right| log\gamma_{\pm} \tag{S11}$$

The effect of the ion activity coefficient in different electrolytes on the potential of Ag/AgI electrode was calculated according to the Nernst equation, here specifically written as:

$$E = E_{AgI/Ag}^{0'} - \frac{RT}{F} \log a_I = E_{AgI/Ag}^{0'} - \frac{RT}{F} \log (\gamma_- c_I)$$
 (S12)

Liquid junction potential calculation:

The liquid junction potentials E_j of the reference electrode of Ag/AgCl/3 M KCl/1 M LiOAc in different sample solutions were calculated by Henderson equation as:

$$E_{j} = \frac{\sum_{j} z_{j} u_{j} (c_{j}^{\beta} - c_{j}^{\alpha})}{\sum_{j} z_{i}^{2} u_{j} (c_{j}^{\beta} - c_{j}^{\alpha})} \frac{RT}{F} \ln \left\{ \frac{\sum_{j} z_{j}^{2} u_{j} c_{j}^{\beta}}{\sum_{j} z_{j}^{2} u_{j} c_{j}^{\alpha}} \right\}$$
(S13)

where the summations involve all ions in the two contacting electrolytes, with negative values for z_j if anions are involved. Phase α denotes the sample solution and phase β the bridge electrolyte.

The potential difference caused by the change of temperature and viscosity of sample solutions:

The diffusion coefficient of iodide is related to the temperature and viscosity of sample solutions, as given by the Stokes-Einstein equation: [7]

$$D_I = \frac{k_B T}{6\pi r_I \eta} \tag{S14}$$

where $k_B = 1.38 \times 10^{-23}$ J/K is the Boltzmann constant, T is the absolute temperature, $r_I = 0.22 \ nm^{[8]}$ is the ion radius of iodide, η is the viscosity of the sample solution. If we take sweat as an example, the viscosity of sweat at 30 °C is between 0.9 to 1.2 cP.^[9] The diffusion coefficient of iodide was calculated to vary between 0.84×10^{-7} dm² s⁻¹ to 1.12×10^{-7} dm² s⁻¹. Applying these values to simulations according to Equation S2 to S5, the reference potential variation caused by viscosity changes in sweat will be around 3.8 mV.

Parameters used for simulation:

 $i = -5 \,\mu\text{A}$, $A = 7 \,\text{mm}^2$, $R = 8.314 \,\text{J mol}^{-1} \,\text{K}^{-1}$, $T = 298 \,\text{K}$, $F = 96485 \,\text{C mol}^{-1}$, $d = 5 \times 10^{-5} \,\text{dm}$, $\Delta t = 0.01 \,\text{s}$.

 $\mathbf{B}_{Nal} = 1.4651, \ \mathbf{B}_{KCl} = 1.2725, \ \mathbf{B}_{NaCl} = 1.4255, \ \mathbf{C}_{Nal} = 0.07233, \ \mathbf{C}_{KCl} = 0.03326, \ \mathbf{C}_{NaCl} = 0.02626.$

 $u_{K^{+}} = 8.00 \times 10^{-4} \text{ cm}^{2} \text{ s}^{-1} \text{ V}^{-1}, \ u_{Cl^{-}} = 8.11 \times 10^{-4} \text{ cm}^{2} \text{ s}^{-1} \text{ V}^{-1}, \ u_{Na^{+}} = 5.47 \times 10^{-4} \text{ cm}^{2} \text{ s}^{-1} \text{ V}^{-1}, \ u_{Li^{+}} = 4.24 \times 10^{-4} \text{ cm}^{2} \text{ s}^{-1} \text{ V}^{-1}, \ u_{OAc^{-}} = 4.38 \times 10^{-4} \text{ cm}^{2} \text{ s}^{-1} \text{ V}^{-1}$

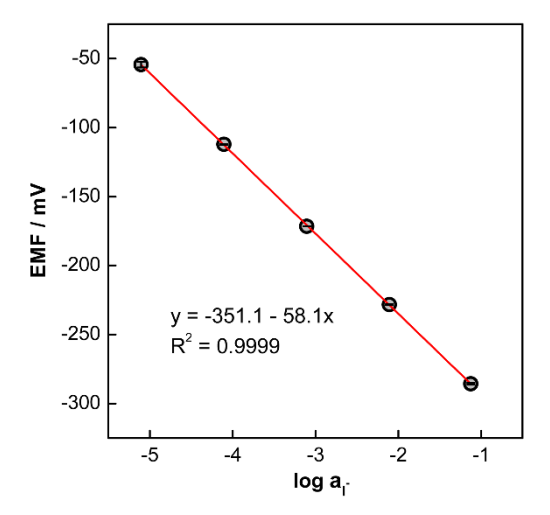


Figure S1. Observed Nernstian response of Ag/AgI electrode to different activities of iodide ions at zero current (n=3). The obtained E⁰ value of -351 mV was used for subsequent simulations.

For the iodide release step, the applied cathodic current density was optimized. The results show that as the amplitude of the applied current increases, the EMF value detected in the second step becomes more negative. For an electrode with a diameter of 3 mm, the electrode gave best stability under the applied current range from -2 μ A to -20 μ A. If the applied current was more negative than -50 μ A, the AgI layer on the Ag electrode was observed to detach from the underlying electrode, giving irreproducible potential readings after 20 or so cycles, see Figure S2.

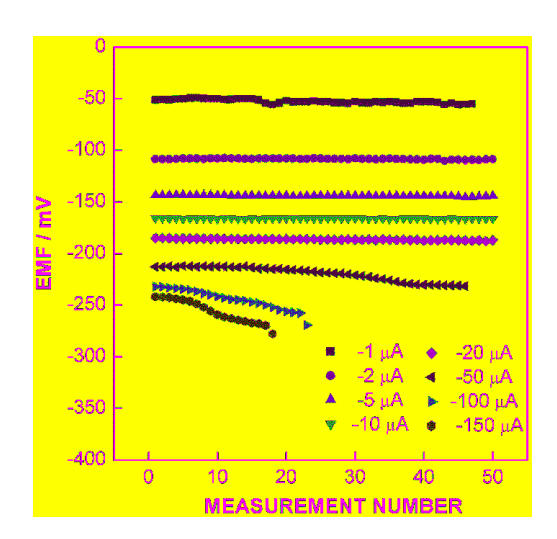


Figure S2. Dependence of the EMF value on the applied current in galvanostatic step. The conditions for the three steps: (I) applying different current from -1 μA to -150 μA for 3 s; (II) detection in 1 s; (III) applying regenerate potential based on the original OCP for 30 s. Background electrolyte: 0.1 M NaCl.

The time of applied current has an influence on the performance of the electrode. As the time increases, the EMF value becomes more negative. The corresponding chronopotentiograms gave rapid potential decreases during the first two seconds, limiting the resulting potential stability. Excessive time should also be avoided because it limits the ability to effectively recapture the iodide ions owing to diffusion into the solution bulk. For this reason, 5 s was applied as the optimum time period at the current of -5 μ A.

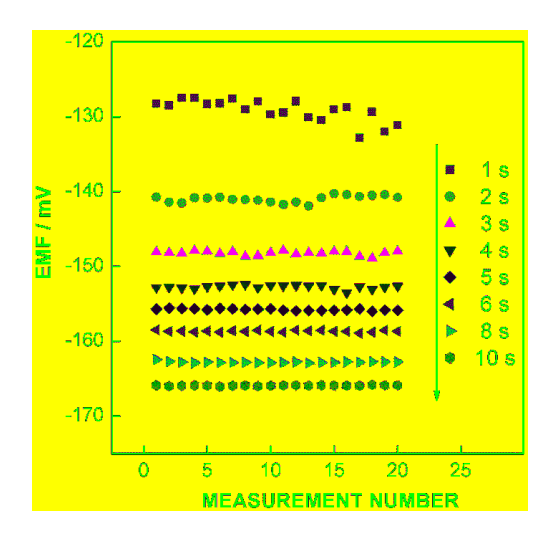


Figure S3. Dependence of the EMF value on the time of the applied current in galvanostatic step. The conditions for the three steps: (I) applying current of -5 μA for different time period; (II) detection in 1 s; (III) applying regenerate potential based on the original OCP for 30 s. Background electrolyte: 0.1 M NaCl.

The effective recapture of iodide into its AgI form is important for long-term stability of the electrode. To regenerate AgI rather than plating additional AgCI in the background electrolyte of NaCI, a potentiostatic pulse was applied. To find the appropriate regeneration potential, a linear sweep voltammogram of the Ag/AgI electrode was recorded in 100 mM of NaCI solution containing 10 mM of NaI, see Figure S4b. A theoretical simulation under the same conditions accompanies the data. In the range from -0.2 V (around the OCP value) to 0.1 V, the iodide plating to AgI is observed while above 0.1 V, chloride ions start to co-deposit as AgCI. Note that the simulated curve does not take into account the ohmic drop of the cell, explaining the difference in slopes. We may conclude that the iodide recapture potential should be at or marginally higher than the original OCP value but lower than the AgCI generation potential. The zero current potential value measured before applying the galvanostatic release step may be used to apply the correct potential for the purpose of recapturing the iodide.

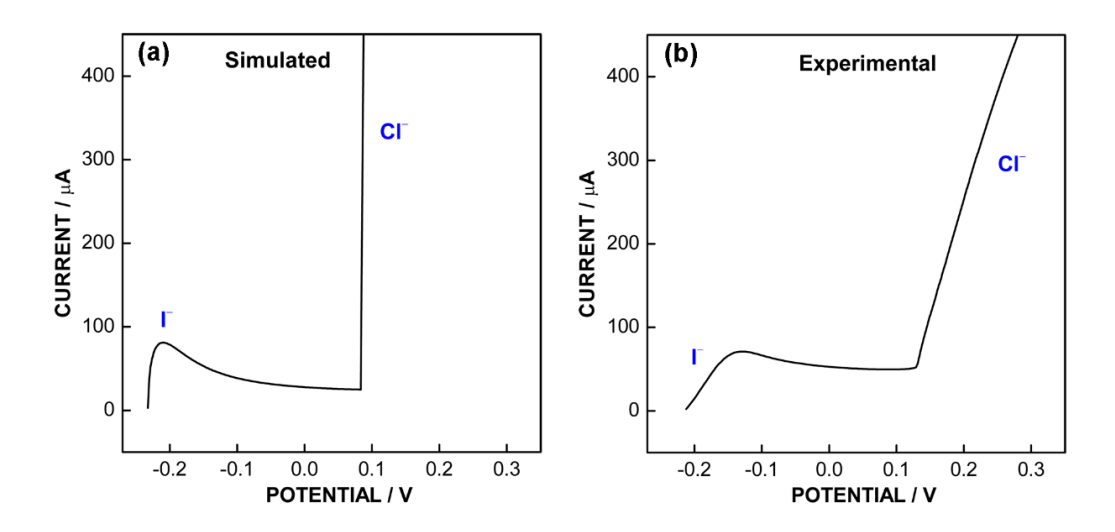


Figure S4. The simulated and experimental linear sweep voltammogram of the Ag/AgI electrode in a solution containing 100 mM of NaCI and 10 mM of NaI.

To find the optimum recapture potential, simulations were made. Under the regeneration potential based on the original OCP value, the standard deviation (SD) of the EMF values is 0.16 mV for 10 consecutive measurements. Increasing the potential to 50 to 150 mV plus the OCP value, the SD is 0.15 mV. A moderate potential increment based on the OCP value improves stability moderately, but a further increase of the potential value did not show more benefits. The experimental measurements gave similar results. Repeated for 50 times, the electrodes showed better stability under the recapture potential of OCP plus 50 mV or OCP plus 80 mV than the OCP value (for which the mean SD of two electrodes is 0.46 mV). Under the recapture potential of OCP plus 50 mV and 80 mV, the mean SD is 0.33 mV and 0.27 mV, respectively, depending on the prepared electrodes. An increment of more than 100 mV was not considered to avoid AgCl plating. For further experiments, the relatively safe value of OCP plus 50 mV was used in the experimental measurements. Some deviations were observed during long time repetitive measurements, which may be due to the accumulation of the released iodide ions in the sample that could not be recaptured. Indeed, the recovery rate was found as 80% from the charge ratio between the iodide release process and the recapture process. The loss of iodide ions is about 0.004% of the whole AgI layer during one repetition. Still, the intermittent potential values are reproducible to less than 1 mV in 50 consecutive measurements, which demonstrates good repeatability. The deviations may be further reduced with a flow system or agitation of the sample after each measurement, which is often applied in real applications. Other methods such as confining the released iodide in some space near the electrode surface may also help the regeneration and extend the lifetime of the electrode.

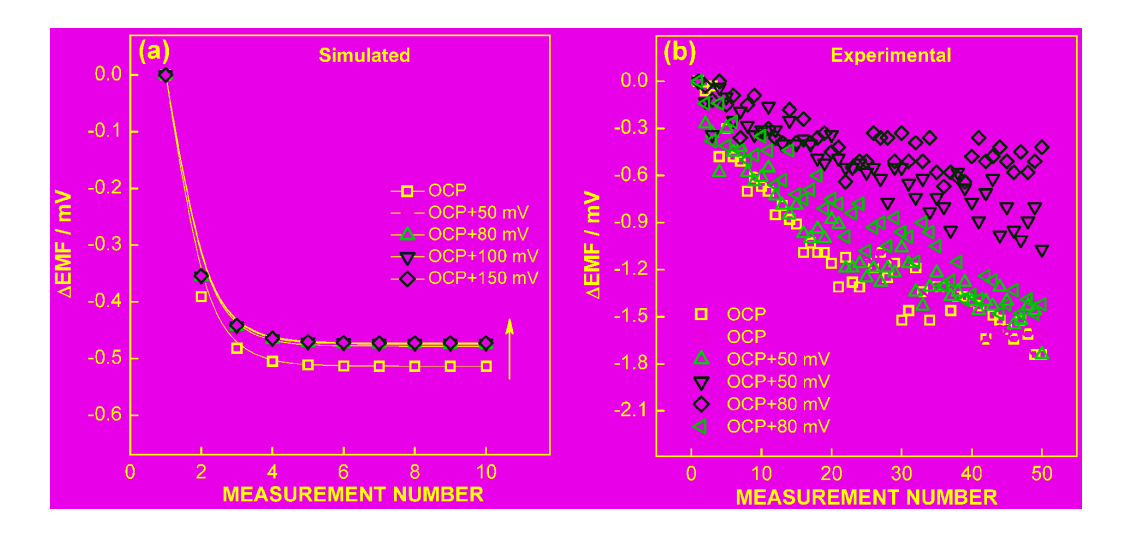


Figure S5. The dependence of Ag/AgI electrode stability on the iodide regeneration potential based on simulated (a) and experimental results (b). The conditions for the three steps: (I) applying current of -5 μA for 5 s; (II) detection in 1 s; (III) applying different regenerate potential for 30 s. Background electrolyte: 0.1 M NaCI.

The regeneration time was also investigated. Simulations were made to show the difference between different regeneration periods from one second to thirty seconds. During 10 consecutive repetitions, the SD of the recorded intermittent potentials decreased from 4.11 mV to 0.15 mV with increasing of the regeneration time. The experimental data showed similar results but the deviations were a few millivolts less than the simulated ones, which may be due to the complex diffusion conditions in the electrochemical cell while a one-dimension diffusion was assumed in simulations. In both cases, 30 s is an attractive regeneration time, which was chosen for subsequent measurements.

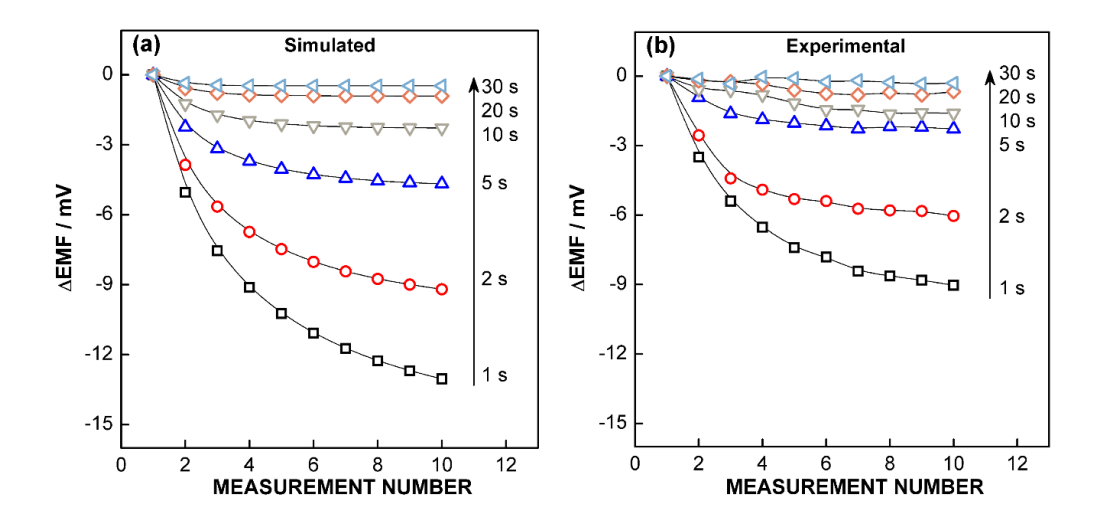


Figure S6. The dependence of Ag/AgI electrode stability on the iodide regeneration time based on simulated (a) and experimental results (b). The conditions for the three steps: (I) applying current of -5 μA for 5 s; (II) detection in 1 s; (III) applying regenerate potential of OCP plus 50 mV for different time period. Background electrolyte: 0.1 M NaCl.

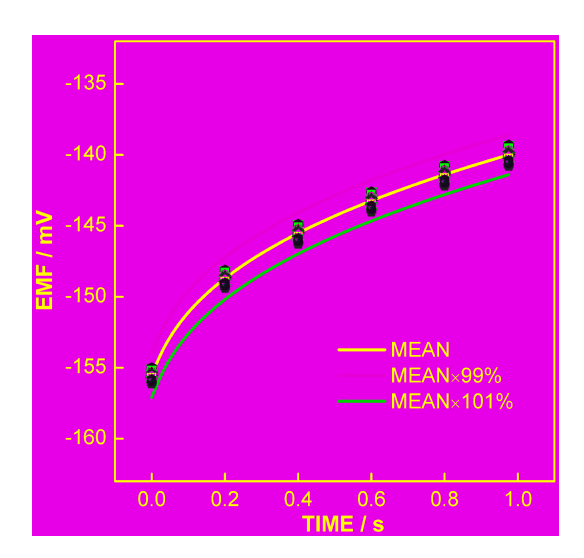


Figure S7. The EMF values measured at open-circuit in one second. The black line is the mean value of 50 times measurements. The red and blue line is the 99% and 101% of the mean value. The data points were extracted at an interval time of 0.2 s in 50 times measurements to show the difference at different time points. Background electrolyte: 0.1 M NaCl.

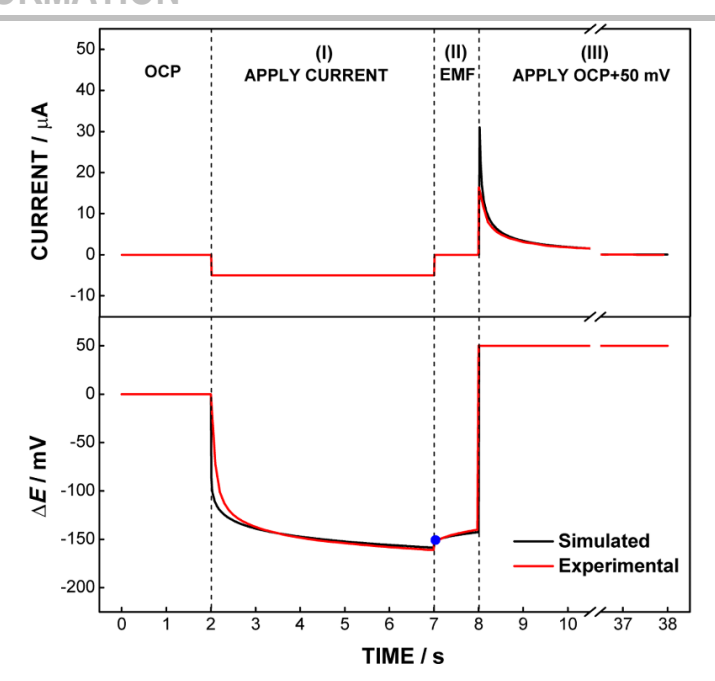


Figure S8. The simulated and experimental curves for the pulse control steps: (I) applying a constant current of -5 μA for 5 s; (II) the EMF measurement in 1 s; (III) applying a constant recapture potential based on the original OCP value of the electrode (OCP plus 50 mV) for 30 s. The first point in step II (the blue point) was used as the data point for analysis.

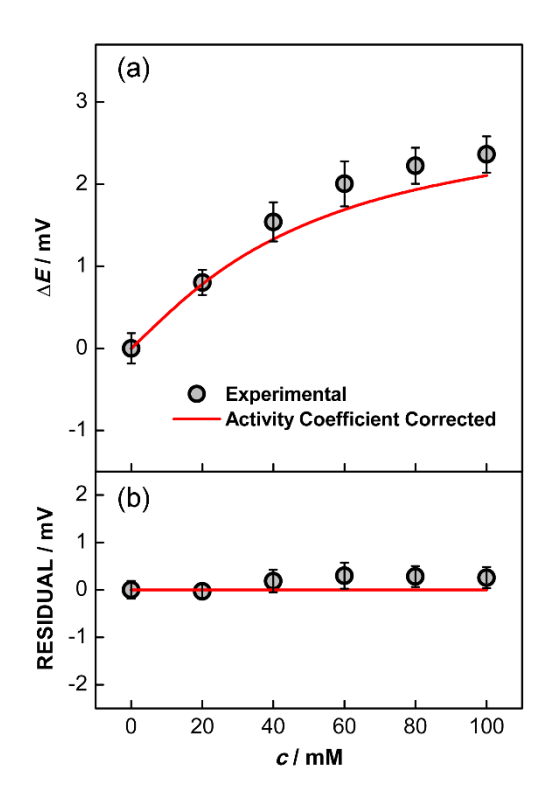


Figure S9. The influence of sulfate on the reference potential of the Ag/Agl pulstrode in 0.1 M NaCl background electrolyte. (a) Experimental potential deviations (n=3) and theoretical potential change (red line) taking into account the change of iodide activity coefficient by increasing the concentration of Na₂SO₄, and (b) the residual values

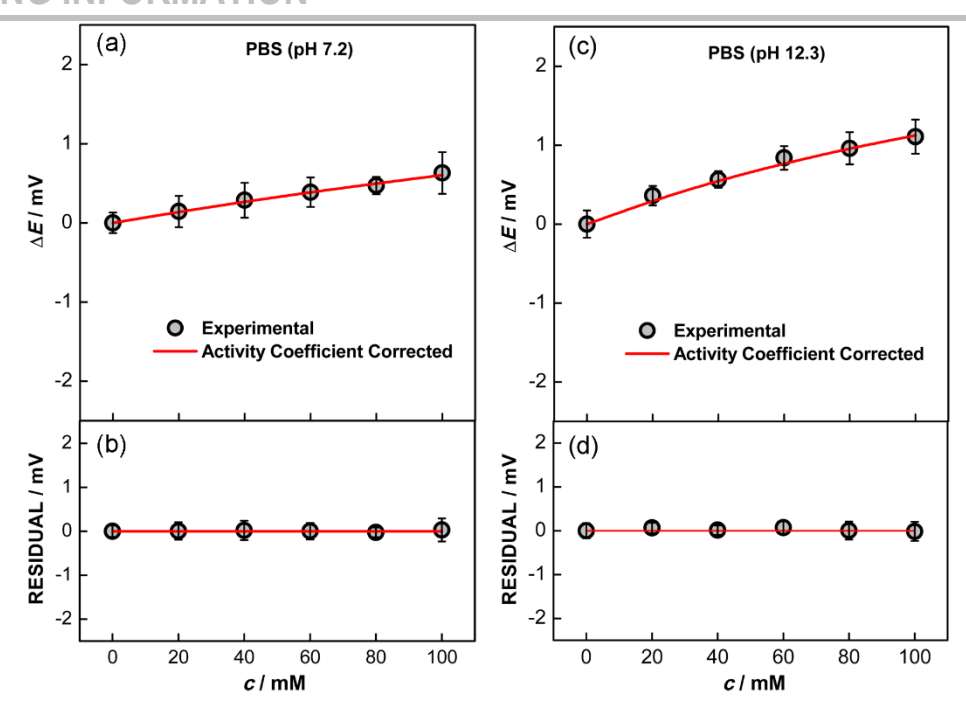


Figure S10. The influence of phosphate species on the reference potential of the Ag/AgI pulstrode in 0.1 M NaCI background electrolyte. Experimental potential deviations (n=3) and theoretical potential change (red line) taking into account the change of iodide activity coefficient by increasing the concentration of phosphate buffer solution (PBS) at pH 7.2 (a) and pH 12.3 (c), and the residual values (b) and (d). The main phosphate species in pH 7.2 PBS are H₂PO₄⁻ and HPO₄²-, in pH 12.3 they are HPO₄²- and PO₄³-, and the molar ratio in both cases is 1:1.

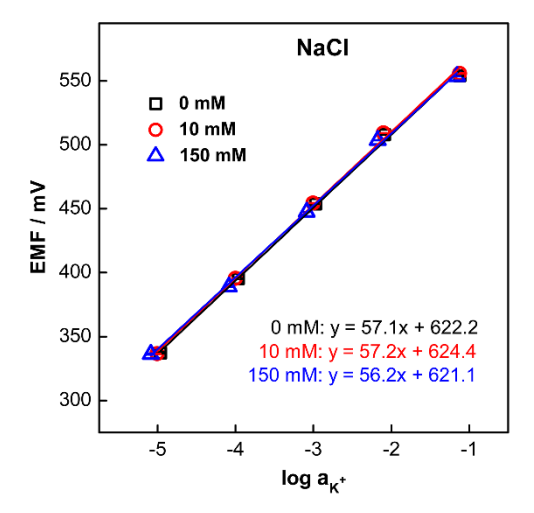


Figure S11. The calibration curves for potassium detection using conventional reference electrode (Ag/AgCl/3 M KCl/1 M LiOAc) in different concentrations of NaCl solutions (n=3). The EMF data were corrected by subtracting the junction potentials calculated according to the Henderson Equation (Eqn. S13).

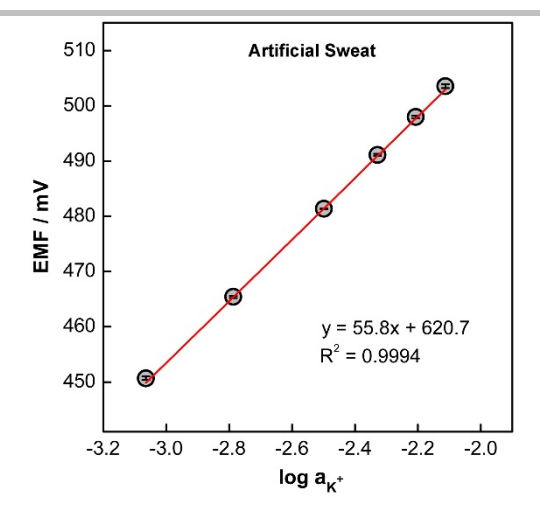


Figure \$12. The calibration curve for potassium based on conventional reference electrode (Ag/AgCl/3 M KCl/1 M LiOAc) in spiked artificial sweat samples (n=3).

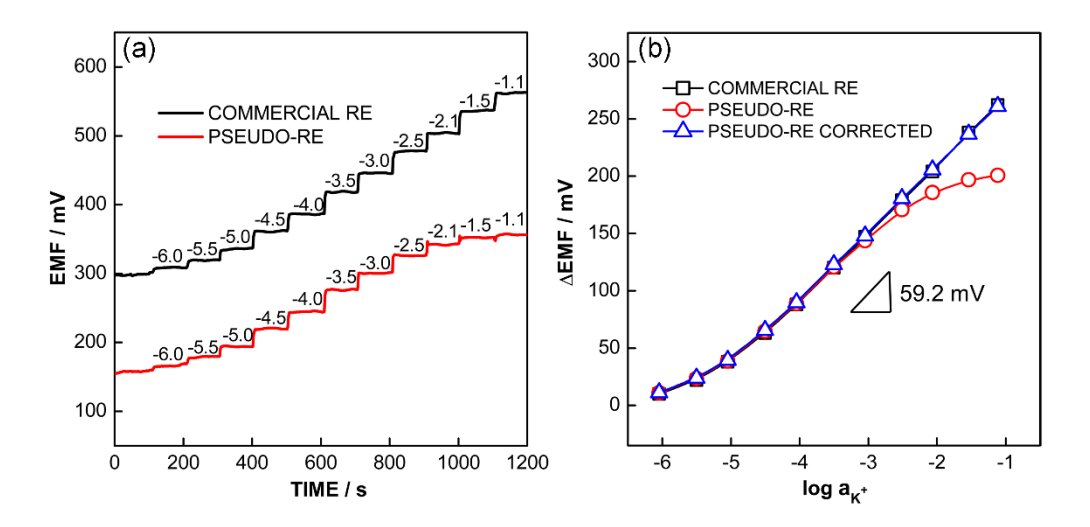


Figure S13. (a) The time responses to KCl additions with a K-ISE as indicator electrode, measured against two different reference electrodes (RE), a commercial Ag/AgCl/3 M KCl/1 M LiOAc electrode (COMMERCIAL RE) and a pseudo-reference electrode consisting of an Ag/AgCl placed behind Nafion membrane (PSEUDO-RE). (b) The calibration curves for potassium using the commercial RE (black trace, square symbols) and pseudo-RE (red trace, circles), and the pseudo-RE readings corrected by the Ag/AgI pulstrode (PSEUDO-RE CORRECTED). Background electrolyte: 10 mM NaCI.

References

- J. Sutter, A. Radu, S. Peper, E. Bakker, E. Pretsch, Anal. Chim. Acta 2004, 523, 53-59.
- G. A. Crespo, G. Mistlberger, E. Bakker, *J. Am. Chem. Soc.* **2012**, 134, 205-207.
 E. Grygolowicz-Pawlak, G. A. Crespo, M. G. Afshar, G. Mistlberger, E. Bakker, *Anal. Chem.* **2013**, *85*, 6208-6212.
 W. Gao, S. Jeanneret, D. Yuan, T. Cherubini, L. Wang, X. Xie, E. Bakker, *Anal. Chem.* **2019**, *91*, 4889-4895.
 D. Yuan, M. Cuartero, G. A. Crespo, E. Bakker, *Anal. Chem.* **2017**, *89*, 586-594.
 P. C. Meier, *Anal. Chim. Acta* **1982**, *136*, 363-368.

- [2] [3] [4] [5] [6] [7]
 - J. Brillo, A. I. Pommrich, A. Meyer, Phys. Rev. Lett. 2011, 107, 165902.
- R. Shannon, Acta Cryst. A 1976, 32, 751-767.
- H. M. Emrich, E. Stoll, B. Friolet, J. P. Colombo, R. Richterich, E. Rossi, Pediat. Res. 1968, 2, 464-478.

Author Contributions

Prof. E. Bakker, Prof. X. Xie and Dr. W. Gao developed the idea, designed the experiments and finished the manuscript writing. Dr. E. Zdrachek provided ideas during discussions and revised the manuscript.